

Exploration of gold nanoparticle beams for matter wave interferometry

Elisabeth Reiger, Lucia Hackermüller, Martin Berninger, Markus Arndt *

Institut für Experimentalphysik, Universität Vienna, Boltzmanngasse 5, A-1090 Wien, Austria

Received 1 November 2005; accepted 7 February 2006

We dedicate this article to Bruce Shore at the occasion of his 70th birthday.

Abstract

We investigate molecular beam methods for gold nanoparticles. They are based on electrospray, matrix assisted laser desorption and thermal laser desorption in combination with mass spectroscopy and multi-photon ionization. These techniques are analyzed with respect to their potential for coherent matter wave experiments.

© 2006 Elsevier B.V. All rights reserved.

Keywords: Matter waves; Molecular beams; Electrospray; Laser desorption

1. Introduction

Over recent years significant progress has been made in the exploration of the wave-particle duality of composite systems such as dimers [1–3], cold helium clusters [4,5] or hot macromolecules [6,7]. In particular large clusters and molecules are interesting for experiments exploring the quantum to classical transition since their internal complexity and thermal state population resembles already largely that of macroscopic classical bodies. The importance of internal properties, such as for instance the polarizability, has already been seen, on a smaller scale, in previous studies of diffraction of atoms and molecules at material gratings [8–10]. The specific internal characteristics were also important in first decoherence experiments with molecules which were recently successfully performed with fullerenes [11,12]. Further studies on the influence of the molecular polarizability, electric and magnetic dipole moments or simply a larger mass and size are of interest in order to trace out the experimental or fundamental limitations for the appearance of quantum effects. For future experiments it is in particular needed to develop novel

sources and detectors. The present article explores three well-established molecular beam methods for one interesting class of particles, namely gold nanocrystals.

In the quest for suitable candidates for interferometry, pure gold nanocrystals are interesting study objects because the physical properties of sufficiently large clusters approach those of bulk metal. And it turns out that their rather low work function and high polarizability are attractive for purely optical coherent manipulation and detection schemes. On the other side, even nanoparticles as small as Au₁₁ can already be imaged and counted in high resolution electron microscopy [13,14]. And the detection will obviously be even easier for larger clusters. This will allow to realize detection schemes reaching an efficiency close to 100% and a spatial resolution of about 1 nm. It is also sometimes argued that matter interferometry will be limited to a certain mass because the diffracted particles still have to pass the opening of the diffracting gratings. For instance, the tobacco mosaic virus ($m \sim 4.5 \times 10^7$), which can also be volatilized in electrospray ionization [15], has a geometric dimension of 18×300 nm [16]. In contrast to that, large gold clusters approach the bulk density of 19.3 g/cm^3 and would be more than ten times smaller than the virus [17]. They would thus still geometrically fit through a narrow grating opening (50 nm). Although all present experiments are still far from this limit the example

* Corresponding author.

E-mail address: Markus.Arndt@univie.ac.at (M. Arndt).

shows that compact metal clusters may have a smaller interaction with their environment than many organic objects, simply because of their size and shape.

Large gold clusters can for instance be obtained from a metal vapor expansion or laser desorption of metallic gold, both in combination with a supersonic expansion in a noble seed gas. These methods typically lead to a large range of cluster sizes. In the present paper we explore the prospects of using ligand-stabilized gold particles, i.e., metal clusters surrounded by a set of organic molecules. Such metal clusters are nowadays routinely prepared in a wet-chemical process. The addition of the organic ligands encloses the metal particles and protects them after a defined growth time in solution against further growth and aggregation. This way a sample of large clusters with a rather well-defined size range can be generated.

We study beams of gold nanoclusters generated by electrospray ionization (ESI), matrix assisted laser desorption ionization (MALDI) and direct thermal laser desorption (TLD). These source methods are complemented by three different detection techniques, namely quadrupole mass spectroscopy (QMS), time-of-flight mass spectroscopy (TOF-MS) and multi-photon ionization (MUPI) TOF-MS. In the final section we will then evaluate all methods with regard to their use in matter wave studies and we propose an experiment for particles in the mass range of 10^6 amu.

2. Ligand-stabilized gold clusters

Certain ligand-stabilized gold clusters [18,19] are expected to be particularly stable and abundant, among them those with 11 or 55 atoms in the metal core. We refer to the first type as ‘undecagold’ and to the second as ‘nanogold’. Our gold nanocrystals were purchased from Nanoprobes Inc. [20] and were used without any further purification. Undecagold is usually described by the formula $\text{Au}_{11}\text{L}_7\text{Cl}_3$ [21,22], in our case with the ligand assignment $\text{L} \equiv \text{PAr}_3 \equiv \text{P}(\text{C}_6\text{H}_4\text{CONHCH}_3)_3$. With this formula it has an isotope averaged mass of 5307 amu.

The geometry and structure of this gold cluster is illustrated in the inset of Fig. 1a. For clarity, only one out of the seven phosphine aryl (PAr) ligands is shown in detail. For the larger ‘nanogold’ the exact number of core atoms is actually not fully controlled by the production. Electron microscopy shows however a metal core diameter of 1.4 nm which is compatible with the assignment to a core of 55 gold atoms [14]. An allowed cluster composition, such as for example $\text{Au}_{55}\text{L}_{12}\text{Cl}_6$, has an isotope averaged mass of $\sim 16,250$ amu. But the production process also allows for a distribution around the mean value by several gold atoms [20].

3. Electrospray ionization

The volatilization of very massive particles is one of the key challenges for future coherent matter wave experiments. While thermal sublimation or the supersonic expansion of gases work very well for some molecules, even up to several thousand atomic mass units [23], it is still technologically demanding to create beams of very massive – and therefore mostly thermolabile – particles. Yet recent developments such as laser desorption and electrospray ionization offer perspectives for experiments on the quantum control of thermolabile molecules, among them most of the organic molecules.

In electrospray ionization (ESI) [24] isolated gas-phase ions are generated from solution by an electrically assisted spray: A solution of analyte molecules, i.e., the ligand-stabilized gold clusters, is filled into a thin capillary in front of the entrance orifice of the vacuum chamber. Applying a high voltage (1–2 kV) between the capillary and the vacuum chamber generates a spray cone which then decomposes into very tiny droplets, mainly because of an imbalance between electrical and hydrostatic forces. Evaporation of the solvent in air causes an electrical instability of the flying droplets which therefore decompose into even smaller off-spring droplets. This solvation and subsequent fission process is repeated several times. While the physics behind the final desolvation mechanism is still not fully

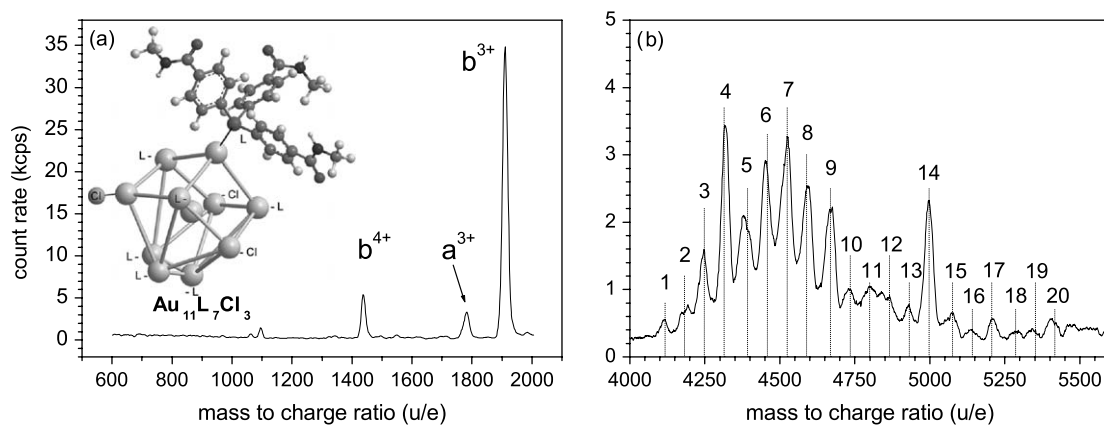


Fig. 1. Quadrupole mass spectra of electrosprayed: (a) undecagold and (b) nanogold ($q = 3+$). Undecagold appears essentially in a single component with a purity of 90% whereas the larger gold nanocrystal is composed of up to 20 different cluster compositions.

agreed on [25], this charge-assisted desolvation is known to be a particularly soft method for fully isolating thermolabile charged particles – in most cases essentially without any fragmentation.

ESI is nowadays a standard tool for the investigation of biomolecules but it also proved useful for large organometallic compounds [26], semiconductor nanocrystals [27–29] and various gold particles [30,31]. The interest of our work in this respect is to characterize the purity of the beam from materials that are readily available as well as to explore the achievable flux. A more detailed description of our experimental setup is given in [32]. Our source is operated with needles with a diameter of 30 μm and flow rates below 1 $\mu\text{l}/\text{min}$. All samples were dissolved in methanol with typical gold crystal concentrations of $c = 1, \dots, 5 \times 10^{-5}$ mol/l. The unsolvated gold nanocrystals are then electrostatically guided by a custom made air/vacuum interface and through two differentially pumped vacuum stages into a high vacuum region, where they can be selected and detected in a quadrupole mass spectrometer (Extrel CMS).

Fig. 1a shows a typical mass spectrum of undecagold. We observe the expected peak of $\text{Au}_{11}(\text{PAR}_3)_7\text{Cl}_3$ (5307 amu) – marked as component (a) – as well as one well-defined peak of much higher intensity (b). Compound (b) is consistent with the cluster compositions $[\text{Au}_{11}(\text{PAR}_3)_8\text{Cl}_2]\text{Cl}$ (5740 amu) and $[\text{Au}_{13}(\text{PAR}_3)_7\text{Cl}_4]$ (5736 amu). In a larger mass scan all charge states from 1+ through 4+ could be observed, but ESI forms neither fragments nor major aggregates, except for a tiny peak at b_2^{3+} . The flux through the quadrupole, integrated over the four charge states, amounts to more than one million mass selected and detected gold particles per second. This flux is for instance sufficiently high to load an ion trap within a few seconds.

Also the larger nanogold crystals can be well volatilized by the electrospray. We identify three charge groups corresponding to 2+ through 4+ within the mass range of our spectrometer. Each single charge group is composed of up to 20 different peaks, as shown in Fig. 1b. The periodic spacing between adjacent peaks is consistent with the addition or subtraction of single gold atoms and/or single

ligands ($L = \text{PAR}_3$). The dotted lines represent possible peak cluster compositions ranging from $\text{Au}_{55}\text{L}_{12}\text{Cl}_6$, for peak (20), to $\text{Au}_{44}\text{L}_8\text{Cl}_6$ for peak (1).

4. Matrix assisted laser desorption

An equally well-established method for volatilizing large thermolabile particles is matrix assisted laser desorption ionization, MALDI [33,34]. Ultraviolet laser light irradiated on a strongly absorbing organic matrix heats the sample in a few nanoseconds, resulting in an abrupt evaporation. The analyte particles, usually supposed to be only weakly absorbing at the laser wavelength, will then also be carried into the gas-phase and even be cooled by the adiabatically expanding matrix.

Since much heat is deposited in the original matrix the survival of the analyte particles depends crucially on their own absorption spectrum. Recent experiments with gold nanocrystals [35,36] showed various degrees of fragmentation depending on the analyte/matrix ratio and the present experiment also aims at studying the number of intact nanocrystals generated using this method. Additional details of our experimental setup can also be found in [32].

We prepare a sample using the dried droplet method [34] and a common MALDI matrix (dihydroxy benzoic acid, DHB). The sample plate is then transferred into a high vacuum desorption chamber where it is irradiated by a pulsed N_2 -laser beam ($\lambda = 337$ nm, 4 ns, 5 Hz, 250 μm) with an energy of 3 μJ . Below this desorption energy no significant ion signal could be observed. The emerging particles are extracted into an orthogonal time-of-flight mass spectrometer (Kaesdorf). Fig. 2a shows the ion mass spectrum for undecagold. The peak labeled with (1) can be attributed to the singly charged intact cluster. The loss of PAR_3 ligands (e.g., $1 \rightarrow 3$) and the successive losses of gold-chlorine complexes (e.g., $1 \rightarrow 2$, $2 \rightarrow 3$) lead to the appearance of 10 fragment peaks. Combination peaks of nanocrystal fragments (4), can also be seen at high masses. The situation is very similar for nanogold, as shown in Fig. 2b.

Although UV-MALDI is a well-established method in protein research, it is obviously more invasive for gold clusters. We attribute this to the plasmon resonance in gold

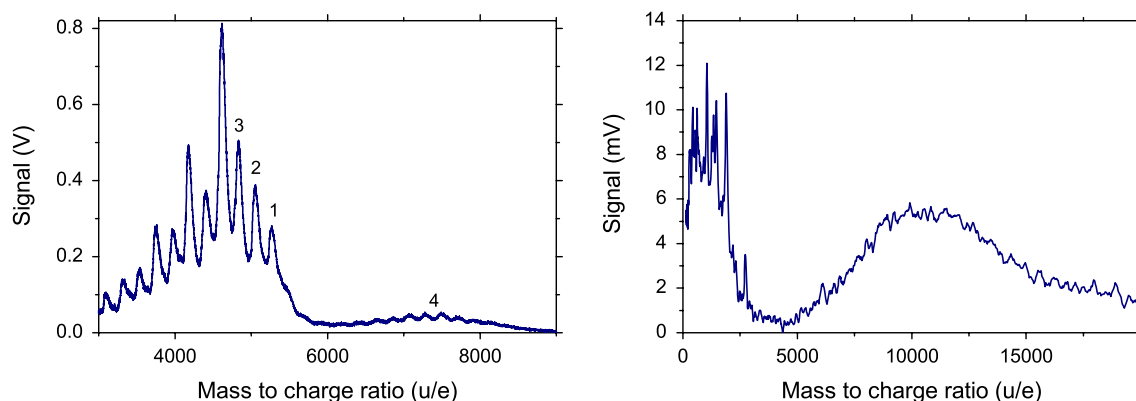


Fig. 2. DHB-MALDI spectra of undecagold and nanogold. Both reveal a strong fragmentation and clustering under UV laser desorption.

which gives rise to strong absorption at the desorption wave length, at least for free gold clusters of similar size [13].

5. Thermal laser desorption

MALDI is known to also produce a significant fraction of neutral particles [37] which would be of immediate interest for quantum interference experiments. But the small analyte concentration as well as the large beam divergence make a detection of neutrals difficult. By omitting the matrix, the gold concentration in the beam can be increased by a factor up to 10,000. For such a *thermal laser desorption* (TLD) the methanol-gold solution is directly dried on the sample plate. The methanol almost completely evaporates, leaving behind a pure layer of ligand-stabilized gold clusters. With the same laser and setup as before TLD now leads to a significant formation of neutral and ligand-free gold clusters ranging from Au_2 to Au_{25} . The highest cluster yield is obtained for a desorption laser intensity around $10 \mu\text{J}$ focused to $200 \mu\text{m}$. We detect the presence of the neutrals by postionizing them with a pulsed Nd-YAG laser (266 nm, 6–8 ns, 1, ..., 4 mJ), which is focused to a spot of about 1 mm diameter at the entrance region of the TOF-MS, located 30 mm behind the desorption region. Fig. 3 shows the mass spectrum of nanogold after thermal laser desorption and postionization. Identical spectra, up to a common scaling factor of 2.4, are observed for undecagold. We do not observe any significant signal beyond 5000 u. In particular there is no signature of clusters with an intact ligand shell. The velocity distribution of the neutral beam is measured by observing the signal strength for varying delay times between the desorption and the ionization laser pulse. From this we deduce typical mean velocities from $v_{\text{mp}} \sim 550 \text{ m/s}$ for the smallest clusters Au_2 to $v_{\text{mp}} \sim 450 \text{ m/s}$ for Au_{13} .

6. Gold clusters for quantum interference experiments?

In general, matter wave physics is experimentally facilitated by using neutral, slow and mass selected particles. Interferometry experiments with electrons and He^+ ions [38–40] show that it is, in principle, also conceivable to imagine interferometry with charged nanogold. But the use of neutral particles eliminates the need of shielding against electro-magnetic perturbations.

Here we shall first briefly assess the status and prospects of the three mentioned beam methods for matter wave interferometry. We have shown above that direct *thermal laser desorption* generates a beam of a large range of ligand-free neutral gold clusters. At present, the signal strength would be sufficient for near-field interferometry with small clusters. For instance for Au_3 ($v \sim 500 \text{ m/s}$) which is comparable in mass to the fullerenes, we expect a signal-to-noise ratio of more than 10 in a few seconds integration time, when they are sent through a Talbot–Lau interferometer composed of three material gratings with a slit period of $g = 257 \text{ nm}$ and a grating separation of $L = 5 \text{ cm}$ which is close to the Talbot length $L_T = g^2/\lambda_{\text{dB}}$. In about this distance the interfering clusters will create a first self-image of the second grating which can be detected by help of the third grating [2,9]. The intrinsic velocity selection in these experiments would always be of the order of one percent, determined by the interferometer length and the width of the ionizing laser pulse. In this scheme, the mass selection would be performed in the detection stage. For significantly larger gold clusters a slowing and cooling scheme should be added (see below). *Matrix assisted laser desorption* also allows to volatilize ligand-stabilized gold. But it generates neither pure nor monodisperse particles and therefore it seems not to be useful for our purposes. Thirdly, as shown above, *electrospray ionization* is a minimally invasive technique for

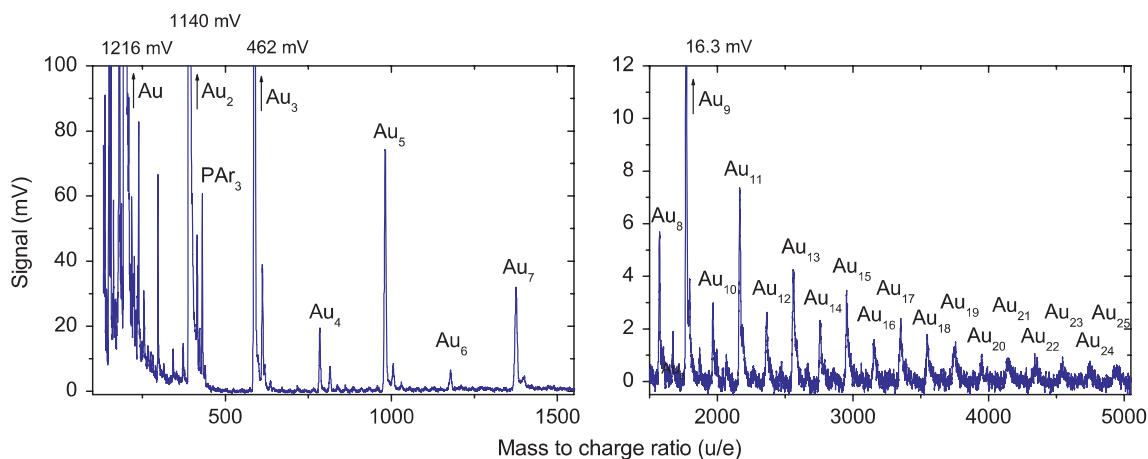


Fig. 3. Mass spectrum of nanogold after photo-ionization (2.8 mJ) of the thermally desorbed neutral beam. This picture is also representative for undecagold, which shows an identical mass spectrum up to an overall amplitude factor. One can clearly identify pure gold clusters, completely stripped of all ligands.

volatilizing gold nanoparticles and it permits to prepare beams of rather well size-selected large and charged nanocrystals.

An important motivation for using metal clusters as matter waves would be the possibility to manipulate their charge state by intense, pulsed VUV laser light. The ionization energy of nanosized gold approaches the work function of the bulk metal, 5.4 eV [41]. Ionization can therefore already be reached by a single photon with a wavelength shorter than 225 nm. For 10^6 amu gold clusters the absorption cross section at this wavelength amounts to about $2 \times 10^{-14} \text{ cm}^2$ [42]. A pulsed ArF (193 nm) or F₂ (157 nm) laser beam would allow to saturate the single photon ionization. It is interesting to see that single photon excitation would also open the way to *absorptive* optical gratings based on either neutralization or ionization and in addition on the optical dipole force. These gratings can then be arranged in a Talbot–Lau interferometer which

is well-suited to explore the interference of very massive particles.

The idea of the proposed experiment is displayed in Fig. 4 and we start by discussing the coherent control of the cluster beam which we assume to be prepared in an ion trap such that all clusters are mass selected ($\sim 10^6$ amu), singly negatively charged, cold (15 K) and therefore thermally slow (~ 0.5 m/s).

The first standing VUV light wave could then act as a neutralization grating for negatively charged gold clusters [42]. Electron detachment by absorption of a single photon can softly neutralize the clusters in the anti-nodes of the standing light wave. Only the neutrals would be retained in the interferometer, whereas the ions will be extracted in a homogeneous field. Fig. 4 illustrates the principle without yet being drawn to scale. The momentum transfer in this process corresponds to the absorption of a single photon. As the initial cluster beam arrives without any

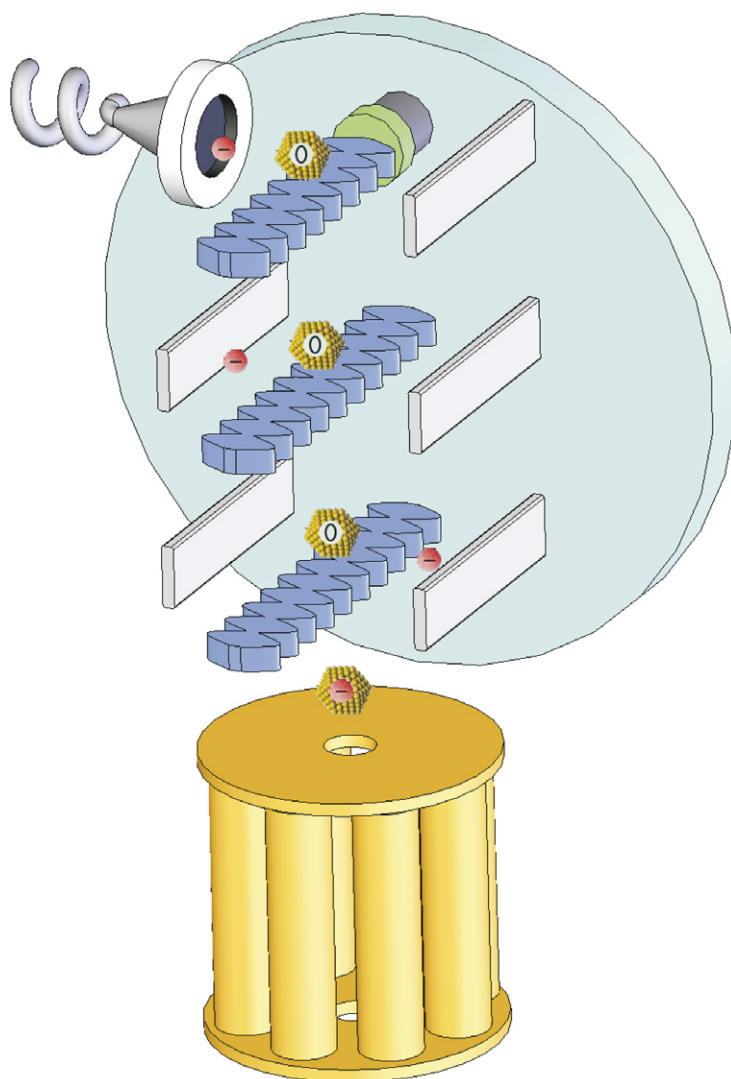


Fig. 4. Setup of the proposed Talbot–Lau interferometer for gold clusters in a mass range up to 1,000,000 amu. The standing laser light waves act as absorptive gratings by either neutralizing or ionizing the cluster beam.

particular collimation the additional photon is of no relevance to the contrast. The very purpose of the first absorptive grating would be to prepare the required spatial coherence of the cluster beam at the position of the second grating by selecting a comb of initial molecular positions.

Multi-photon absorption is of no major concern here, although it may occur. It will only modify the count rate, not the interference contrast. A second or even more absorbed photons would take the cluster into a positive charge state. And also these ions will be extracted by the first set of electrodes. The first optical grating would thus prepare a neutral beam with increased spatial coherence, as required for matter wave interference.

We propose to use the same laser wavelength to implement a second optical grating which will have both an absorptive (ionizing) and a phase (dipole force) part. The relative contribution of both may be chosen within certain limits by varying the laser intensity: at high optical powers photo-ionization becomes relevant, and only clusters in the anti-nodes will move on as neutrals, while the ions will be extracted in a homogeneous field. At low laser intensity the second grating may be used as a pure transmission phase grating, exploiting the dipole interaction between the laser field and the high polarizability of the metal clusters (up to $\sim 5 \text{ \AA}/\text{atom}$).

In both cases, diffraction at the second grating leads to a periodic cluster density distribution in about the Talbot distance downstream. In this position a last VUV light pulse would then allow to ionize the remaining neutrals, again in an optical absorptive grating which is spatially commensurate with the particle density pattern and thus suitable for scanning and imaging the interferogram [9]. Scanning could be performed with a piezo controlled mirror directly glued onto the principle mirror for utmost stability.

The use of such optical absorptive gratings would eliminate many problems at the same time. In contrast to material gratings, they are of utmost precision and reproducibility. They cannot be mechanically destroyed, molecules cannot ‘touch’ their walls, and they avoid van der Waals interactions – which turn out to be otherwise very influential in macromolecule interferometry [9]. In addition the grating alignment can be extremely stable, if all light beams are reflected off the same mirror substrate as shown in Fig. 4.

It is a particular advantage of metal clusters over organic molecules, that such optical absorptive gratings are conceivable. Many organic particles would either require multi-photon ionization, which would be incompatible with the coherence requirements for interferometry, or rather fragment than ionize [43] the particles. It is a further positive aspect of using clusters with high atomic numbers, that the third grating could be substituted by a surface onto which the clusters are adsorbed for later imaging in high resolution electron microscopy.

Based on these considerations we can now consider an experiment, which can turn ESI, and possibly also TLD,

into a source for far-reaching quantum interferometry studies. The complete experimental sequence will require at least four steps: the volatilization of negatively charged pure gold nanoparticles, their loading into a cooling ion trap, interference in an optical Talbot–Lau interferometer and finally the detection.

Electrospray beams of size-selected nanogold are clearly feasible, as we have shown above. And the removal of the ligand shell in an oxygen plasma has recently been demonstrated by [17]. The interaction with the plasma would have to be set to obtain a final charge state of $q = -1$. Although this has, to our knowledge, not yet been explicitly studied, it appears reasonable to assume that the charge state can be manipulated by the parameters of the plasma, such as the electron density or the interaction time. The guiding of singly charged anions through several differential pumping stages is rather straightforward and already implemented in our setup. It should be extended by another bending ion guide and another vacuum stage to ensure that all unwanted residual materials and gases are separated from the mass selected ion beam. The pure gold clusters can then be captured and cooled in a buffer gas loaded cryogenic multipole ion trap. Such devices are nowadays routinely used for spectroscopy of small molecules [44], where temperatures as low as 15 K have been measured. Alternatively, one may also employ thermal laser desorption close to the buffer gas cooled trap, this time using nanoparticles with diameters of up to 2 nm on the substrate. This has been shown to prepare pure gold cluster up to at least 10^5 amu , and it might lead even further [45].

Once cooled, the gold cluster anions will have to be electrically shifted out of the trap, towards the interferometer, which starts by the electron detachment grating. As mentioned above, at 15 K, the thermal velocity of particles in the 10^6 amu mass range amounts to only 0.5 m/s, corresponding to a de Broglie wavelength of 0.8 pm which is only about a factor of five smaller than in previous fullerene experiments [6,9]. Because of the small optical grating constant, which is determined by half the wavelength of the F_2 -laser beam, i.e., 78.5 nm, the Talbot length amounts to less than one centimeter! Various technical reasons, related to the cluster beam divergence or alignment requirements, may stretch this by an order of magnitude. But still the proposed interferometer appears to be rather compact and appealing, once a cold trap of pure massive gold clusters is established.

The orientation of the interferometer will have to be chosen according to the fine details of the experiment. In a horizontal arrangement, the interferometric phase shifts due to earth’s gravity and rotation, will either require a dedicated compensation by placing the experiment on a suitably oriented turn-table or a velocity selection to better than 0.1% to avoid phase averaging. In a vertical arrangement the dephasing effects can be strongly reduced, but at the expense of a de Broglie wavelength which changes during the propagation. For very massive and slow particles this will require a careful choice of the grating distances.

The third grating could however also be completely eliminated and replaced by a clean cold or specifically prepared surface which will adsorb and immobilize the slowly arriving massive clusters. The use of either electron or scanning probe microscopy would then allow to image any arbitrary period of the adsorbed cluster pattern.

Every step of our outlined proposal has already been either described in the literature or partially been realized in our lab. And although the combination of all parts still poses an significant technological challenge, the requirements appear not to be insurmountable. The various open issues concerning the decoherence of objects in this size regime are an additional motivation for these studies. A realization of our proposal has the potential of pushing the current experimental limits of matter wave interferometry by several orders of magnitude.

Acknowledgements

This work has been supported by the FWF projects STARTY177 and F1505, the Vienna Hochschuljubiläumstiftung as well as by the European Commission under Contract No. HPRN-CT-2002-00309. We acknowledge the contribution of Julia Stroebele in the early stage of our ESI experiments.

References

- [1] M.S. Chapman, T.D. Hammond, A. Lenef, J. Schmiedmayer, R.A. Rubenstein, E. Smith, D.E. Pritchard, *Phys. Rev. Lett.* 75 (1995) 3783.
- [2] J.F. Clauser, S. Li, *Phys. Rev. A* 49 (1994) R2213.
- [3] C. Bordé, N. Courtier, F.D. Burck, A. Goncharov, M. Gorlicki, *Phys. Lett. A* 188 (1994) 187.
- [4] W. Schöllkopf, J.P. Toennies, *Science* 266 (1994) 1345.
- [5] R. Bruehl, R. Guardiola, A. Kalinin, O. Kornilov, J. Navarro, T. Savas, J.P. Toennies, *Phys. Rev. Lett.* 92 (2004) 185301.
- [6] M. Arndt, O. Nairz, J. Voss-Andreae, C. Keller, G.V. der Zouw, A. Zeilinger, *Nature* 401 (1999) 680.
- [7] L. Hackermüller, S. Uttenthaler, K. Hornberger, E. Reiger, B. Brezger, A. Zeilinger, M. Arndt, *Phys. Rev. Lett.* 91 (2003) 90408.
- [8] R. Brühl, P. Fouquet, R.E. Grisenti, J.P. Toennies, G.C. Hegerfeldt, T. Köhler, M. Stoll, C. Walter, *Europhys. Lett.* 59 (2002) 357.
- [9] B. Brezger, L. Hackermüller, S. Uttenthaler, J. Petschinka, M. Arndt, A. Zeilinger, *Phys. Rev. Lett.* 88 (2002) 100404.
- [10] O. Nairz, M. Arndt, A. Zeilinger, *Am. J. Phys.* 71 (2003) 319.
- [11] K. Hornberger, S. Uttenthaler, B. Brezger, L. Hackermüller, M. Arndt, A. Zeilinger, *Phys. Rev. Lett.* 90 (2003) 160401.
- [12] L. Hackermüller, K. Hornberger, B. Brezger, A. Zeilinger, M. Arndt, *Nature* 427 (2004) 711.
- [13] J.F. Hainfeld, R.D. Powell, *J. Histochem. Cytochem.* 48 (2000) 471.
- [14] G. Schmid, R. Pugin, T. Sawitowski, U. Simon, B. Marler, *Chem. Commun.* 14 (1999) 1303.
- [15] B. Bothner, G. Siuzdak, *Chem. BioChem* 5 (2004) 258.
- [16] W. Shenton, T. Douglas, M. Young, *Adv. Mater.* 11 (1999) 253.
- [17] F. Schulz, S. Franzka, G. Schmid, *Adv. Funct. Mater.* 12 (2002) 532.
- [18] W. Jahn, *J. Struct. Biol.* 127 (1999) 106.
- [19] J.D. Aiken, R.G. Finke, *J. Mol. Catal. A* 145 (1999) 1.
- [20] <http://www.nanoprobes.com>.
- [21] P. Bellon, M. Manassero, M. Sansoni, *J. Chem. Soc., Dalton Trans.* 14 (1972) 1481.
- [22] P.A. Bartlett, B. Bauer, S. Singer, *J. Am. Chem. Soc.* 100 (6) (1978) 5085.
- [23] P.J. Fagan, *Science* 262 (1993) 404.
- [24] J.B. Fenn, M. Mann, C.K. Meng, S.F. Wong, C.M. Whitehouse, *Science* 246 (1989) 64.
- [25] R.B. Cole, *Electrospray Ionization Mass Spectrometry*, Wiley, New York, 1997.
- [26] J.C. Traeger, *Int. J. Mass Spectrom.* 200 (2000) 387.
- [27] T. Løver, W. Henderson, G.A. Bowmaker, J.M. Seakins, R.P. Cooney, *Inorg. Chem.* 36 (1997) 3711.
- [28] J.-J. Gaumet, G.F. Strouse, *J. Am. Soc. Mass Spectrom.* 11 (2000) 338.
- [29] J.J. Gaumet, G.A. Khitrov, G.F. Strouse, *NanoLetters* 2 (2002) 375.
- [30] H.-F. Zhang, M. Stender, R. Zhang, C. Wang, J. Li, L.-S. Wang, *J. Phys. Chem. B* 108 (2004) 12259.
- [31] Y. Negishi, K. Nobusada, T. Tsukuda, *J. Am. Chem. Soc.* 127 (2005) 5261.
- [32] M. Arndt, L. Hackermüller, E. Reiger, *Braz. J. Phys.* 35 (2005) 216.
- [33] K. Tanaka, H. Waki, Y. Ido, S. Akita, Y. Yoshida, T. Yoshida, T. Matsuo, *Rapid Commun. Mass Spectrom.* 2 (1988) 151.
- [34] M. Karas, F. Hillenkamp, *Anal. Chem.* 60 (1988) 2299.
- [35] E. Gutierrez, R.D. Powell, F. Furuya, J.F. Hainfeld, T. Schaa, M. Shagullin, P. Stephens, R.L. Whetten, *Eur. Phys. J. D* 9 (1999) 647.
- [36] T.G. Schaaff, R.L. Whetten, *J. Phys. Chem. B* 104 (2000) 2630.
- [37] C.D. Mowry, M.V. Johnston, *Rapid Commun. Mass Spectrom.* 7 (1993) 569.
- [38] C. Davisson, L. Germer, *Nature* 119 (1927) 558.
- [39] F. Hasselbach, U. Maier, *Quantum Coherence and Decoherence, ISQM, Tokyo, 1998*, 299.
- [40] D.L. Freimund, K. Aflatooni, H. Batelaan, *Nature* 413 (2001) 142.
- [41] D. Lide (Ed.), *CRC Handbook of Chemistry and Physics*, 79th ed., 1998–1999.
- [42] V. Kasperovich, V.V. Kresin, *Phil. Mag. B* 78 (1998) 385.
- [43] K.P. Aicher, U. Wilhelm, J. Grottemeyer, *J. Am. Soc. Mass Spectrom.* 6 (1995) 1059.
- [44] D. Gerlich, *Phys. Scr. T59* (1995) 256.
- [45] I. Vezmar, M.M. Alvarez, J.T. Khoury, B.E. Salisbury, M.N. Shafiqullin, R.L. Whetten, *Z. Phys. D* 40 (1997) 147.